Semi-Annual Report

to the

National Aeronautics and Space Administration

Langley Research Center

from

Research Institute of Colorado

Contract #NAG-1-150

"Radiation Budget Measurement/Model Interface Research"

Thomas H. Vonder Haar, Principal Investigator

with Contributions from:

Paul Cieslelski
David Randel
Duane Stevens
Thomas Vonder Haar

with Technical Monitor

G. Louis Smith, NASA, LaRC

October, 1981

Research Institute of Colorado
Drake Creekside Two, Suite 200 2625 Redwing Fort Collins, Colorado 80526 (303) 226-6003

CONTENTS

FIGURE CAPTIONS

Fig. 1-1 Global maps (i.e., I.R. emitted flux, net flux, and albedo) of processed NIMBUS-6 data for July, 1977. Units for fluxes (watts/m^2), for albedo (percent).

Fig. 1-2 Same as 1, except for August, 1977.

Fig. 1-3 Same as 1, except for September, 1977.

Fig. 1-4 Same as 1, except for October, 1977.

Fig. 1-5 Same as 1, except for November, 1977.

Fig. 1-6 Same as 1, except for December, 1977.

Fig. 1-7 Same as 1, except for January, 1978.

Fig. 1-8 Same as 1, except for February, 1978.

Fig. 1-9 Same as 1, except for March, 1978.

Fig. 1-10 Same as 1, except for April, 1978.

Fig. 1-11 Same as 1, except for May, 1978.

Fig. 1-12 Scale and geography for global maps (i.e., Figs 1-11)

Fig. 1-13 Zonal averages of net radiation flux for April.

Fig. 1-14 Same as 1-12, except for May.

Fig. 1-15 Same as 1-12, except for June.

Fig. 1-16 Zonal mean emitted flux (watts/m^2) for Dec - Jan period

Fig. 1-17 Zonal mean net flux (watts/m^2) for Dec - Jan period

Fig. 2-1 Net solar radiation at the surface and top of the model's atmosphere for January

Fig. 2-2 Observed and calculated mean zonal wind 500 mb

Fig. 2-3 Observed (200 mb) and calculated (250 mb) mean zonal wind

Fig. 2-4 Observed (700 mb) and calculated (750 mb) meridional wind

Fig. 2-5 Observed and calculated pressure velocity ω 500 mb

Fig. 2-6 Calculated precipitation and mixing ratio day 91-120

SUMMARY

During the first seven months of research on Radiation Budget Measurement/Modeling Interface we have laid plans and completed early work in three areas: (a) Improved Earth Radiation Budget Data Sets, (b) Numerical Model Experiment Definition and (c) Review of Concurrent Research by Other Scientists. All of these areas of work will be reported in detail via special reports now in preparation. Figures included in the following sections of the present report illustrate the work in progress.

1.0 Improved Earth Radiation Budget Data Sets

As a guide to selection of climate modeling experiments we are continuing our early work by processing and analyzing the NIMBUS-6 data. The first two years of NIMBUS-6 data as well as earlier data, which have been previously processed, were reported by Stephens *et al.* (1981). In recent months we completed the processing of the third year of NIMBUS-6 data. Unfortunately, the data quality from June, 1978 through October, 1978 was insufficient to provide a meaningful analysis of the earth's radiation budget for this period. Thus, the third year of data extends from July, 1977 to May, 1978. The processed results for the "third year" of the NIMBUS-6 data are shown in Figures 1-1 through 1-11. The scale and geography for these global maps is shown in Figure 12. These data are being combined with earlier data (see Table 1) to form the most up-to-date climatology of the earth's radiation budget from which the model work noted below will be guided. Special attention has been directed to the April - June period, which is hypothesized by the P. I. to be a principal time of potential interannual variability in the radiation budget.

From the processed data generated from the satellites referenced in Table 1, we have computed the zonal averages of net radiation for the three months mentioned above (Figures 1-13 through 1-15). It is still uncertain whether the differences observed in these zonal averages are, in fact, manifestations of an interannual variability within the earth's radiation budget, or if they are merely artifacts of the various satellite sampling systems.

Assuming satellite problems to be minimal, the Northern Hemisphere winters of 1975/76, 1976/77 and now 1977/78 are particularly interesting. In contrast to Campbell (1981) who surmised only minor differences between 75/76 and 76/77, our preliminary results from this research show 75/76 and 77/78 to be strikingly similar in terms of radiation budget - with 76/77, the winter of major North

Figure 1-1

18/ 7/ 77

MAX 350.00 INC 20.000 W/M**2 FLUX 1

MES-236.567-236.567 GLB-235.397-235.397

TR ASSEND INVRS 15 DECON

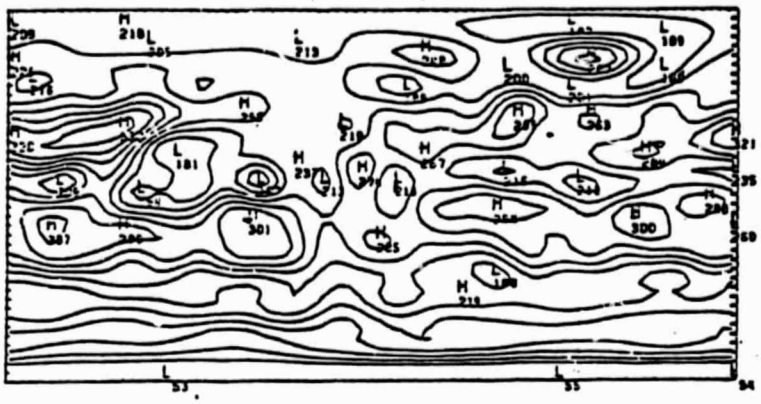

MAX 300.00 INC 20.000 W/M**2 FLUX 8

MES -.941 -.930 GLB -.198 -.198

NET FROM EM DEC 15 ALLDDEC 15

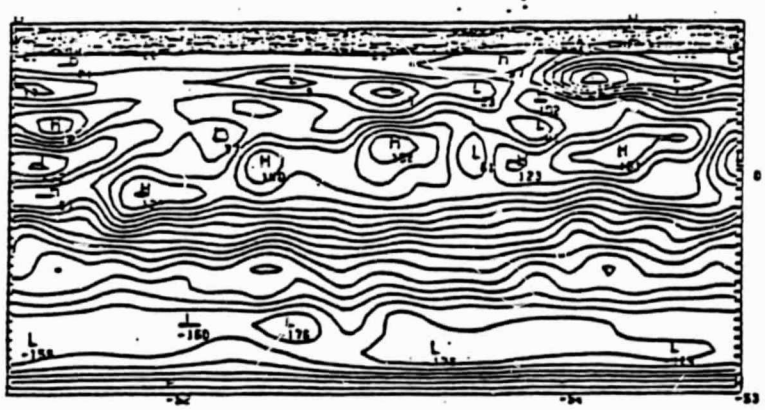

MAX 100.00 INC 5.0000 W/M**2 FLUX 4

MES .293 97.796 GLB .293 97.489

DAILY AVERREF ASSENDLANDMD SAT

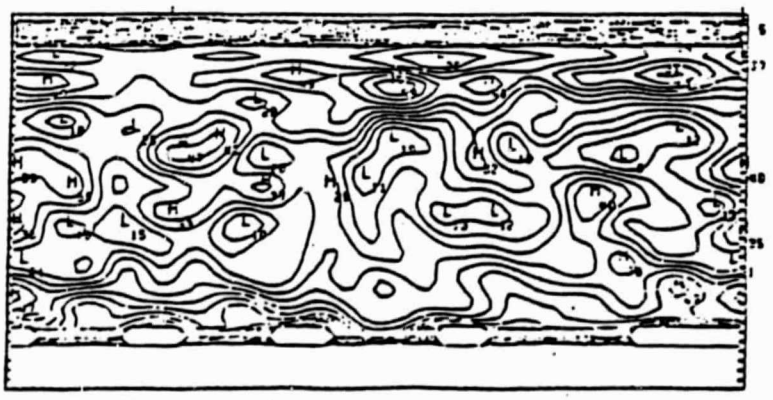

Figure I-2

18/ 8/ 77

MAX 350.00 INC 20.000 W/M**2 FLUX 1

MES-235.316-235.316 GLB-234.137-234.137

IR ASSEND INVRS 15 DECON

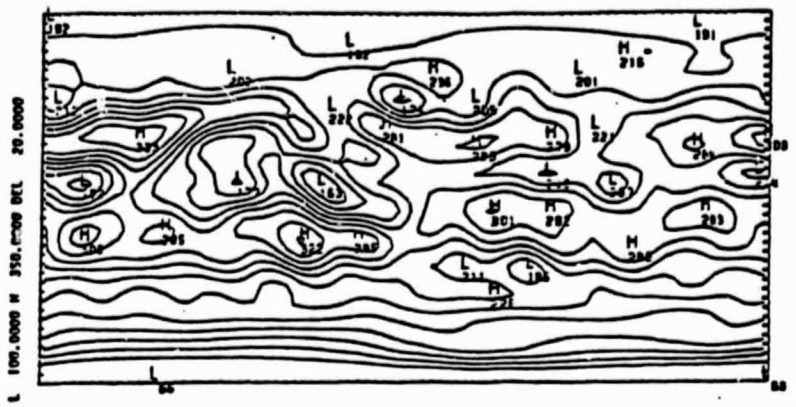

MAX 100.00 INC 5.0000 W/M**2 FLUX 4

MES .287 96.959 GLB .286 96.064

DAILY AVERREF ASSENDLANDMD SAT

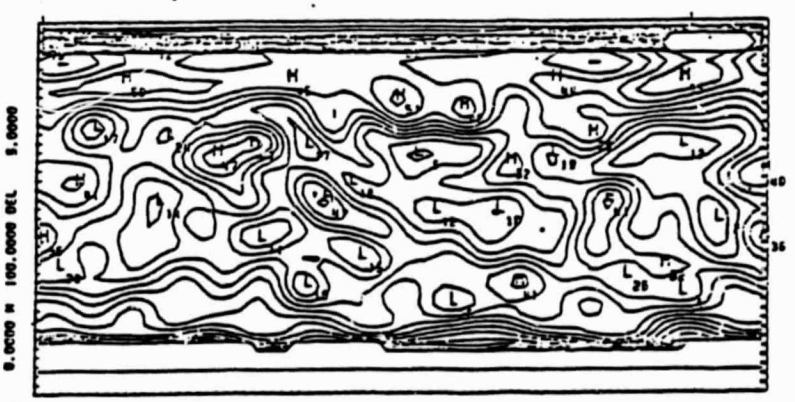

MAX 300.00 INC 20.000 W/M**2 FLUX 8

MES 4.935 4.875 GLB 5.244 5.244

NET FROM EM DEC 15 ALLDDEC 15

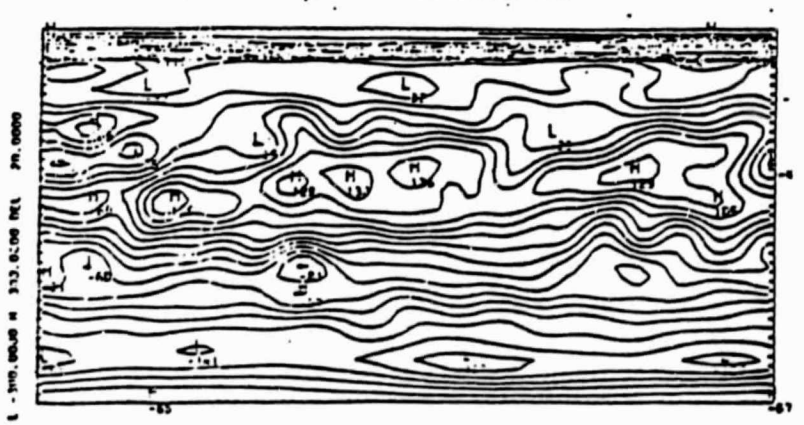

Figure I-3

17/ 9/ 77

MAX 350.00 INC 20.000 W/M**2 FLUX 1
MES-233.586-233.586 GLB-232.278-232.278
IR ASSEND INVRS 15 DECON

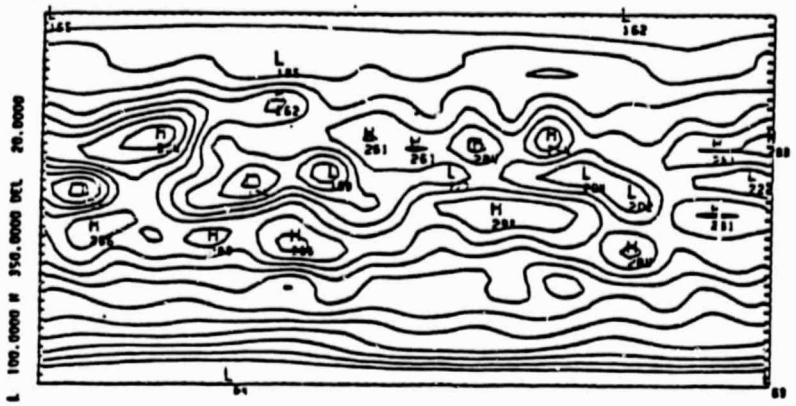

MAX 100.00 INC 5.0000 W/M**2 FLUX 4
MES .288 99.171 GLB .288 98.155
DAILY AVERREF ASSENDLANDMD SAT

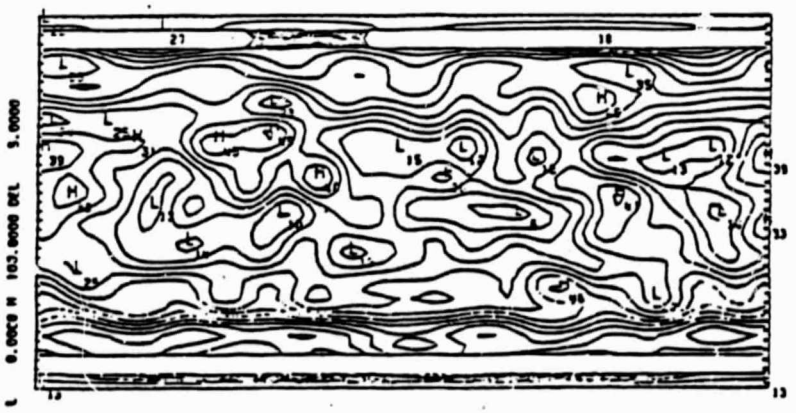

MAX 300.00 INC 20.000 W/M**2 FLUX 8
MES 11.294 11.155 GLB 10.482 10.482
NET FROM EM DEC 15 ALLDDEC 15

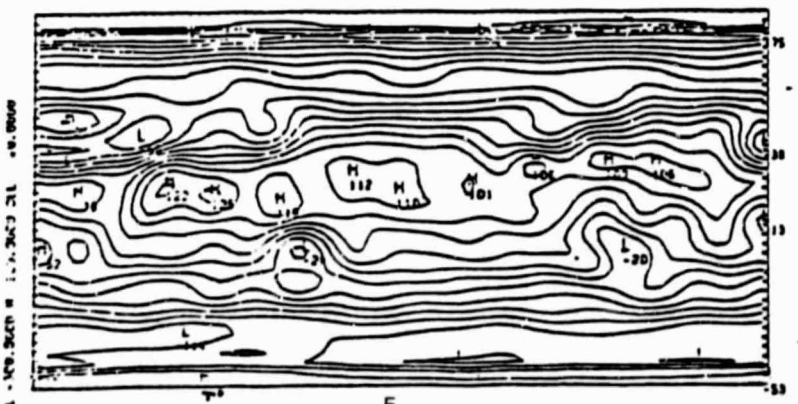

Figure I-4

18/10/ 77

MAX 350.00 INC 20.000 W/M**2 FLUX 1
MES-229.668-229.668 GLB-228.630-228.630
IR ASSEND INVRS 15 DECON

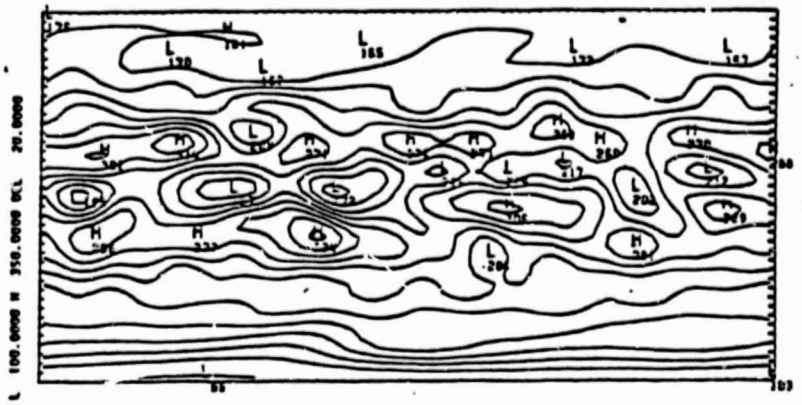

MAX 100.00 INC 5.0000 W/M**2 FLUX 4
MES .299 104.529 GLB .302 104.514
DAILY AVERREF ASSENDLANDMD SAT

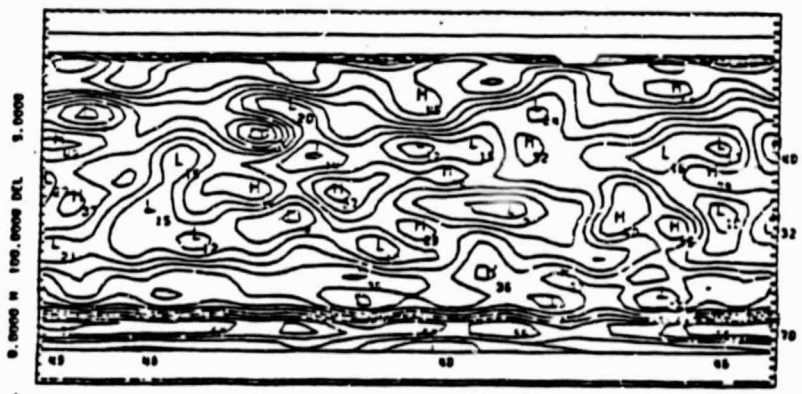

MAX 300.00 INC 20.000 W/M**2 FLUX 8
MES 15.161 14.974 GLB 13.905 13.905
NET FROM EM DEC 15 ALLDDEC 15

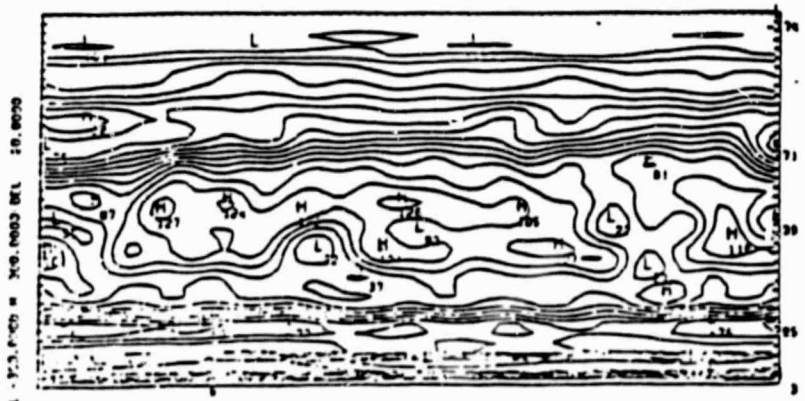

Figure I-5

17/11/ 77

MAX 350.00 INC 20.000 W/M**-2 FLUX 1
MES-225.777-225.777 GLB-225.133-225.133
IR ASSEND INVRS 15 DECON

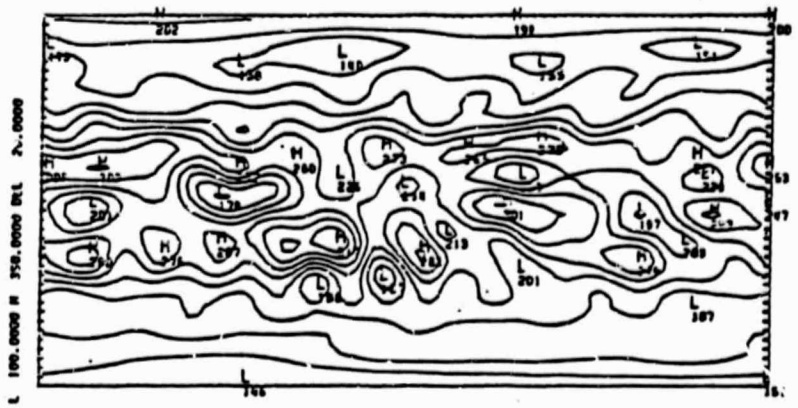

MAX 100.00 INC 5.0000 W/M**2 FLUX 4
MES .311 109.718 GLB .317 111.636
DAILY AVERREF ASSENDLANDMD SAT

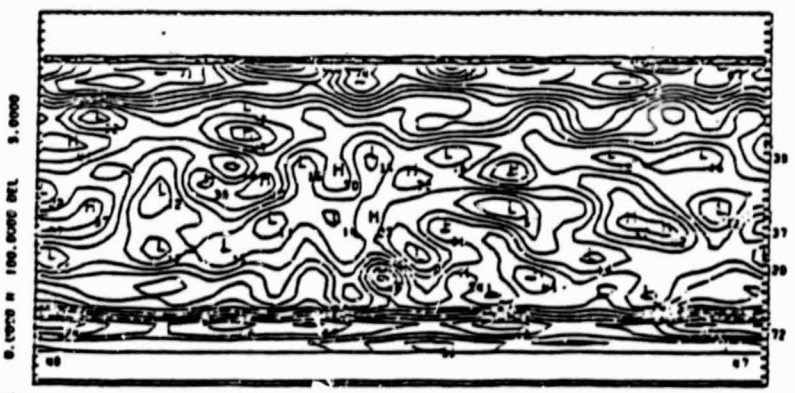

MAX 300.00 INC 20.000 W/M**2 FLUX 8
MES 18.135 17.912 GLB 16.739 16.739
NET FROM EM DEC 15 ALLDDEC 15

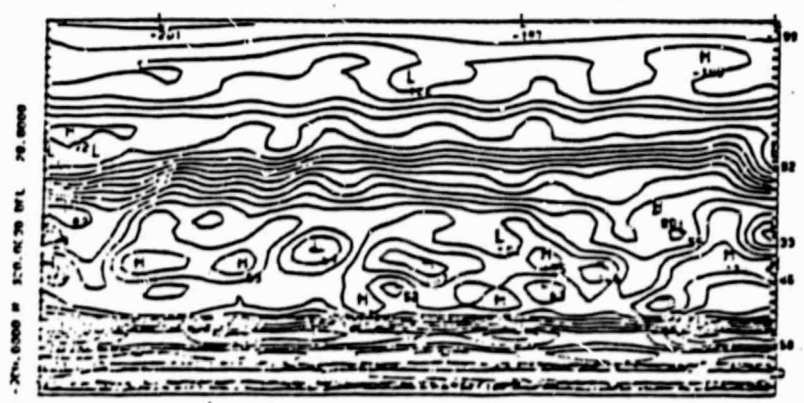

Figure I-6

18/12/ 77

MAX 350.00 INC 20.000 W/M**2 FLUX 1
MES-224.262-224.262 GLB-223.799-223.799
IR ASSEND INVAS 15 DECON

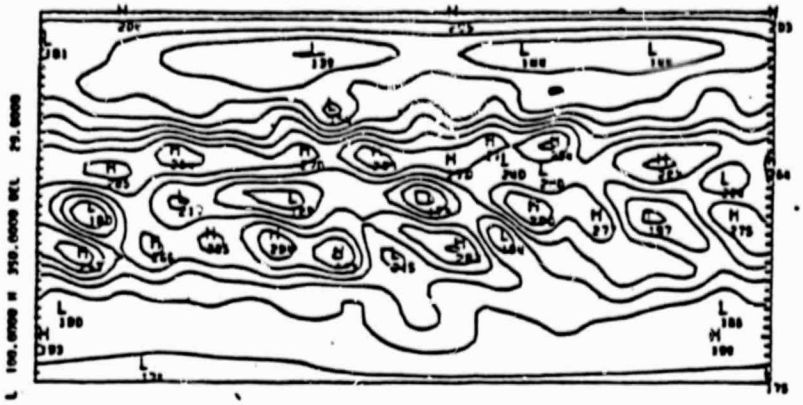

MAX 100.00 INC 5.0000 W/M**2 FLUX 4
MES .313 111.394 GLB .322 114.171
DAILY AVERREF ASSENDLANDMD SAT

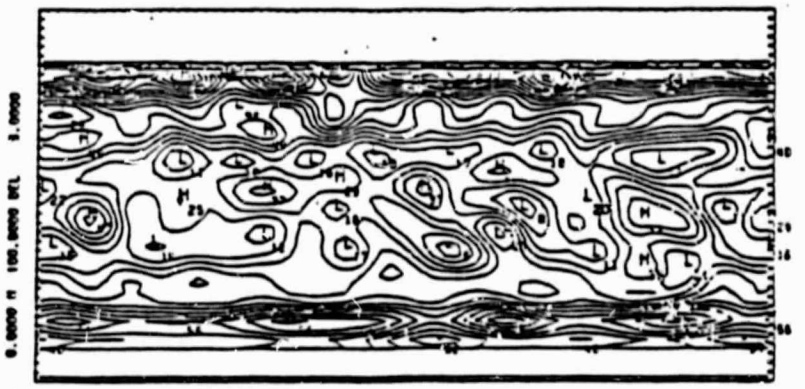

MAX 300.00 INC 20.000 W/M**2 FLUX 8
MES 20.614 20.360 GLB 19.164 19.164
NET FROM EM DEC 15 ALLDDEC 15

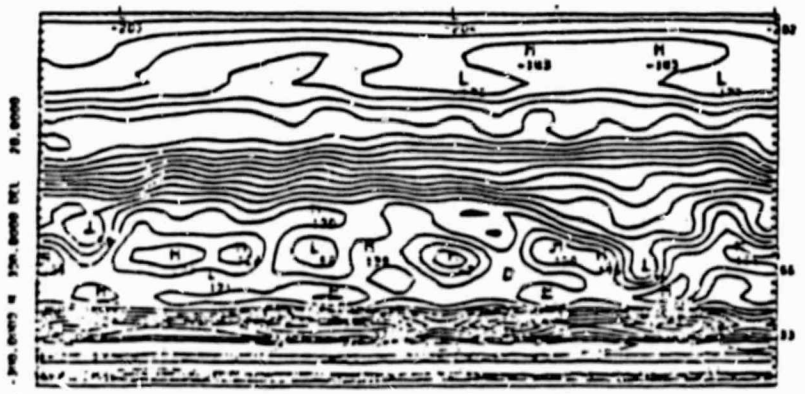

Figure I-7

18/ 1/ 78

MAX 350.00 INC 20.000 W/M**2 FLUX 1

MES-226.111-226.111 GLB-225.582-225.582

IR ASSEND INVRS 15 DECON

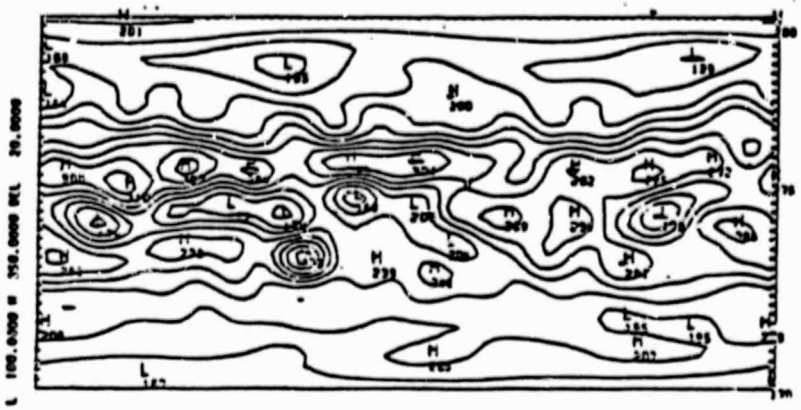

MAX 100.00 INC 5.0000 W/M**2 FLUX 4

MES .305 108.752 GLB .313 111.066

DAILY AVERREF ASSENDLANDMD SAT

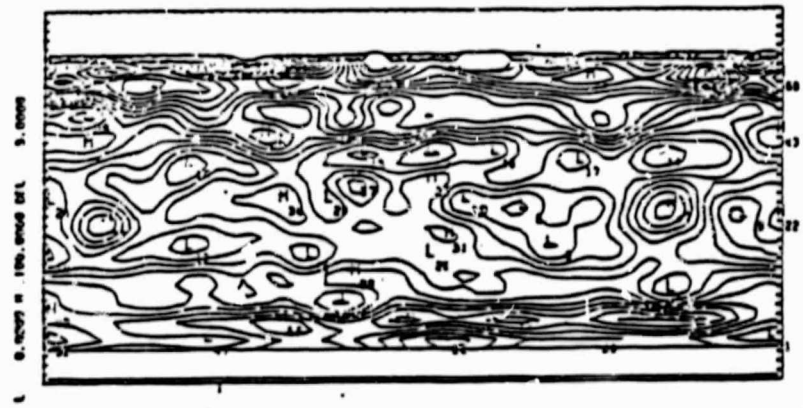

MAX 300.00 INC 20.000 W/M**2 FLUX 8

MES 21.651 21.385 GLB 20.214 20.214

NET FROM EM DEC 15 ALLDDEC 15

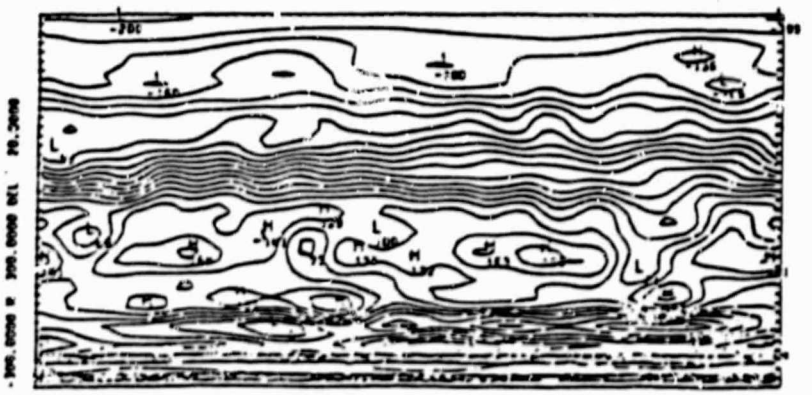

Figure I-8

16/ 2/ 78

MAX 350.00 . INC 20.000 W/M**2 FLUX 1

MES-226.905-226.905 GLB-226.180-226.180

IR ASSEND INVRS 15 DECON

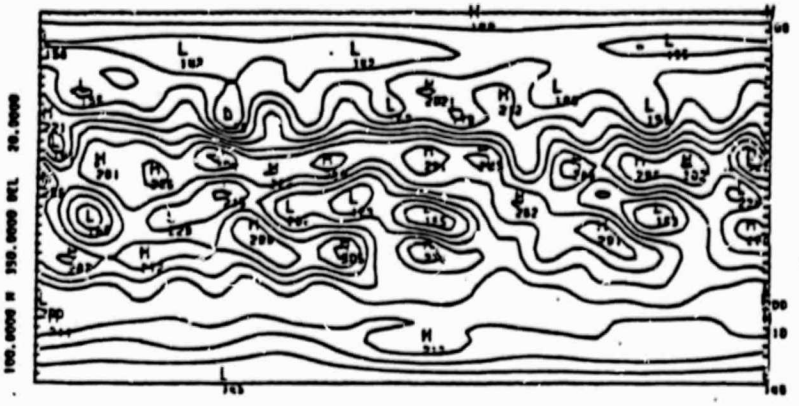

MAX 100.00 INC 5.0000 W/M**2 FLUX 4

MES .301 106.718 GLB .305 107.233

DAILY AVERREF ASSENDLANDMD SAT

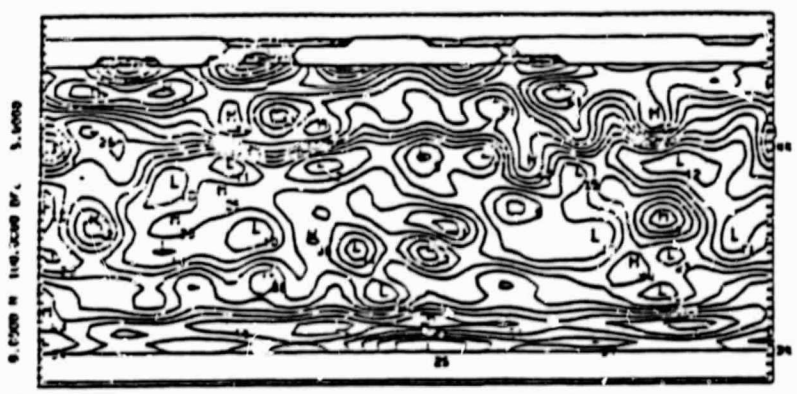

MAX 300.00 INC 20.000 W/M**2 FLUX 8

MES 20.755 20.529 GLB 19.418 19.418

NET FROM EM DEC 15 ALLDDEC 15

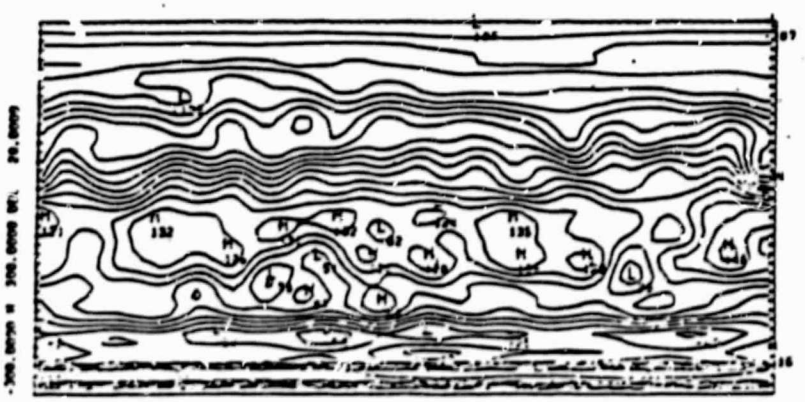

NET 16/ 2/ 78

Figure I-9

18/ 3/ 78

MAX 350.00 INC 20.000 W/M**2 FLUX 1

MES-228.835-228.835 GLB-227.834-227.834

IR ASSEND INVRS 15 DECON

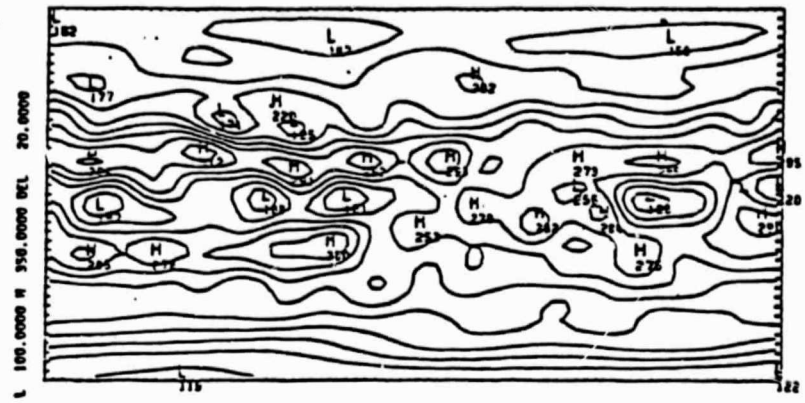

MAX 100.00 INC 5.0000 W/M**2 FLUX 4

MES .298 104.319 GLB . .298 103.421

DAILY AVERREF ASSENDLANDMD SAT

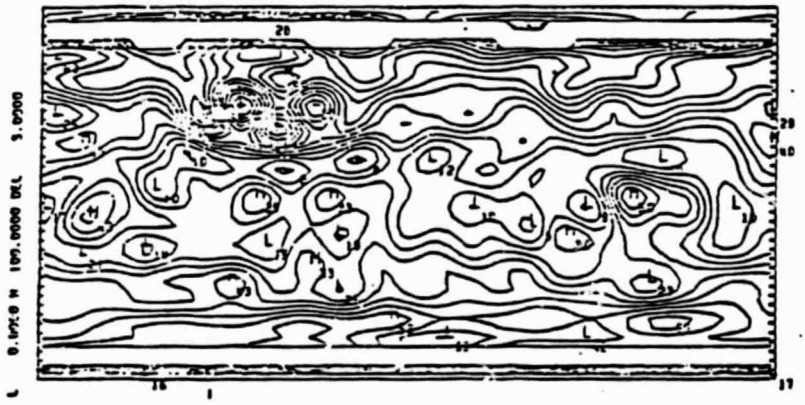

MAX 300.00 INC 20.000 W/M**2 FLUX 8

MES 17.787 17.568 GLB 16.674 16.674

NET FROM EM DEC 15 ALLDDEC 15

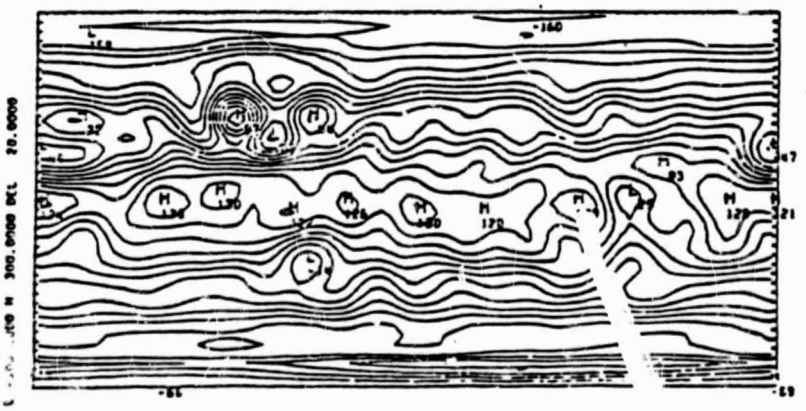

Figure I-10

17/ 4/ 78

MAX 350.00 INC 20.000 W/M**2 FLUX 1

MES 229.824 226.994 GLB 228.693 228.693

IR ASSEND INVRS 15 DECON

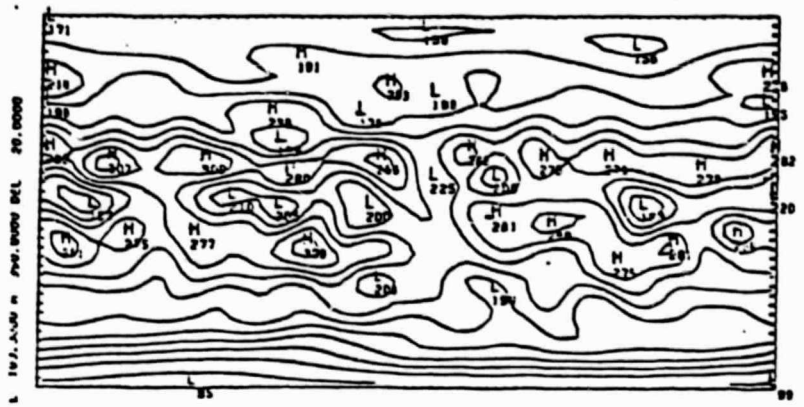

MAX 100.00 INC 5.0000 W/M**2 FLUX 4

MES .326 .322 GLB .324 .324

DAILY AVERREF ASSENDLANDMD SAT

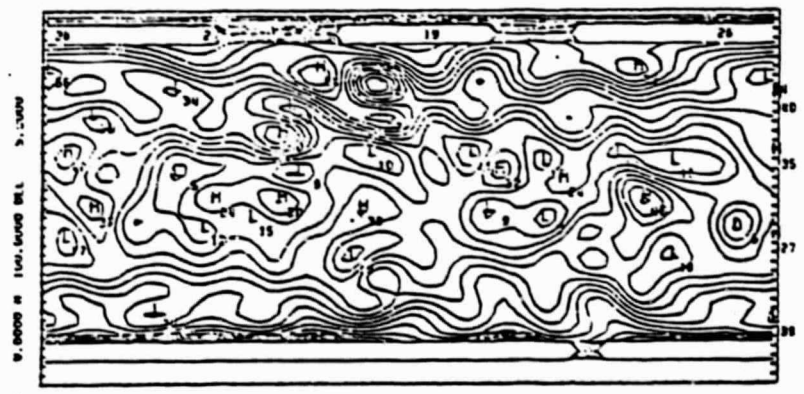

MAX 300.00 INC 20.000 W/M**2 FLUX 8

MES 11.828 11.682 GLB 11.691 11.691

NET FROM EM DEC 15 ALLDDEC 15

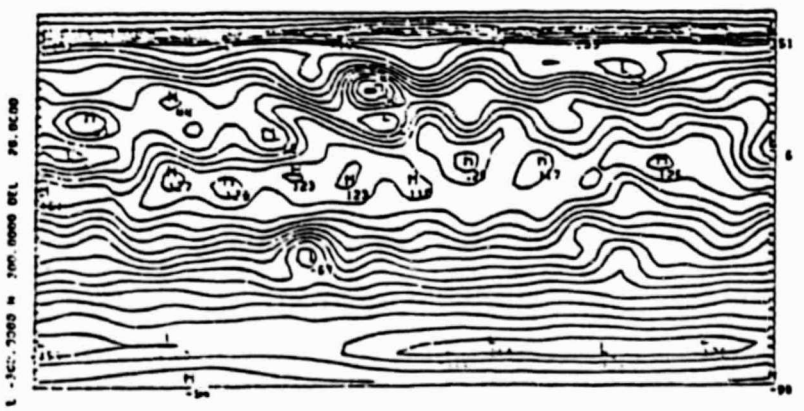

Figure I-11

18/ 5/ 78

MAX 350.00 INC 20.000 W/M**2 FLUX 1
MES-231.836-231.836 GLB-230.803-230.603
IR ASSEND INVRS 15 DECON

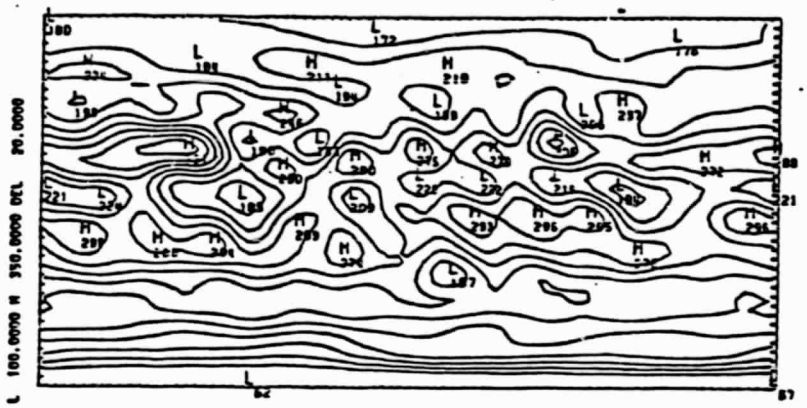

MAX 100.00 INC 5.0000 W/M**2 FLUX 4
MES .302 101.885 GLB .302 101.257
DAILY AVERREF ASSENDLANDMD SAT

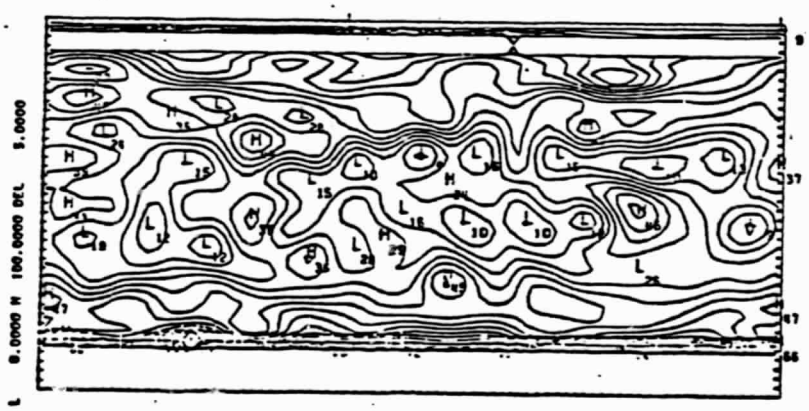

MAX 300.00 INC 20.000 W/M**2 FLUX 8
MES 3.558 3.514 GLB 4.473 4.473
NET FROM EM DEC 15 ALLDDEC 15

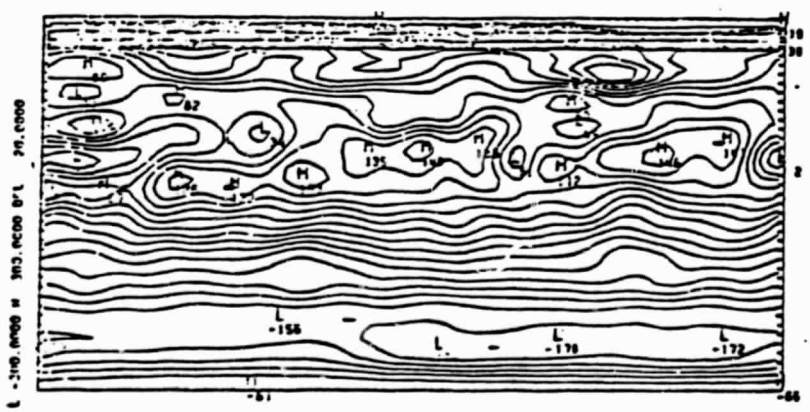

Figure 1-12

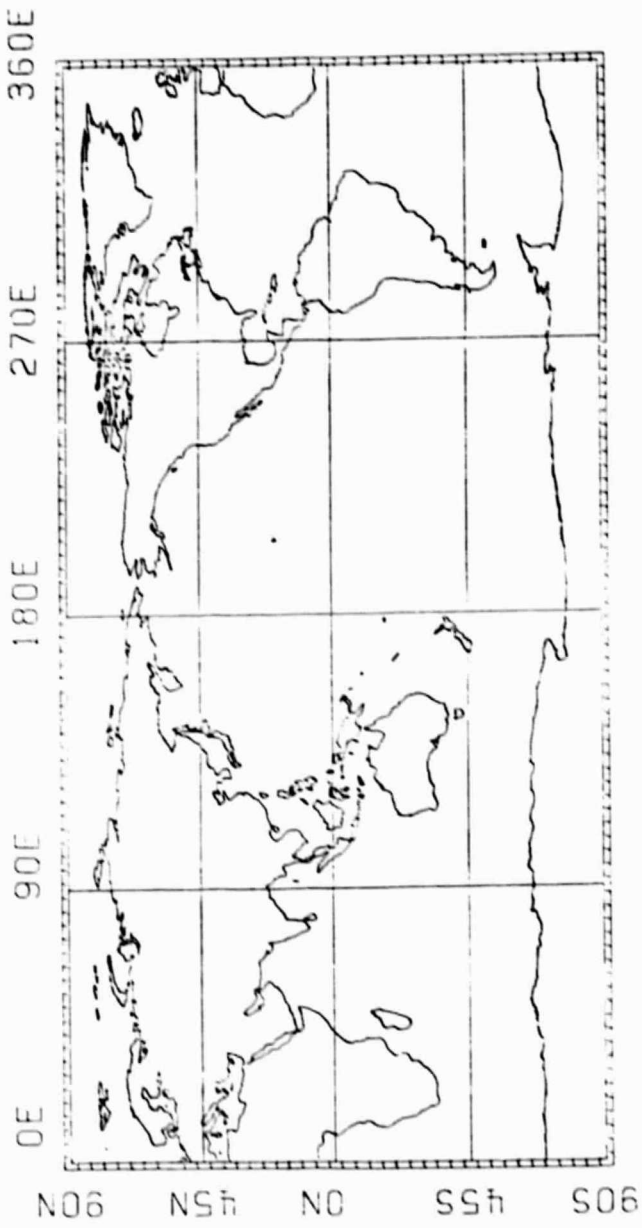

Table 1. Chronological list of earth orbiting satellites from which present radiation measurements were taken. The approximate local time at which each satellite crossed the equator during daylight hours appears in parenthesis. EX - Experimental, N2 - Nimbus 2, N3 - Nimbus 3, N6 - Nimbus 6, E3 - Essa 3 and E7 - Essa 7.

Month	Season	1964	1965	1966	1968	1969	1970	1975	1976	1977	1978	Sample Size
Jan	D.J.F.		Ex(10:30)			E7	N3		N6	N6	.	6
Feb			Ex(10:35)			E7			.	N6	.	5
Mar			Ex(10:40)			E7			.	N6	.	5
Apr	M.A.M.					N3(11:30)*			.	N6	.	4
May						N3			.	N6		4
Jun				N2(11:30)*		N3			.	N6		4
Jul	J.J.A.	Ex(8:30)				N3		N6(11:45)*	.	.		5
Aug		Ex(8:55)				N3		N6	.	.		5
Sep		Ex(9:15)						N6	.	.		4
Oct	S.O.N.	Ex(9:40)			E7(14:30)	N3		N6	.	.		6
Nov		Ex(10:05)			E7			N6	.	.		5
Dec	D.J.F.	Ex(10:30)		E3(14:40)	E7			N6	.	.		6
Annual		6	3	2	3	9	1	6	12	12	5	59

Resolution = Half Power Diameter

Experimental	1280 km, 11.5°
ESSA3	
Nimbus 2	Averaged to 10° grid
ESSA7	2200 km, 20°
Nimbus 3	Averaged to 10° grid
Nimbus 6	1100 km, 10° (analyzed from 16°

*Albedo corrected for diurnal variation of reflection with directional reflectance model.

Figure 1-13

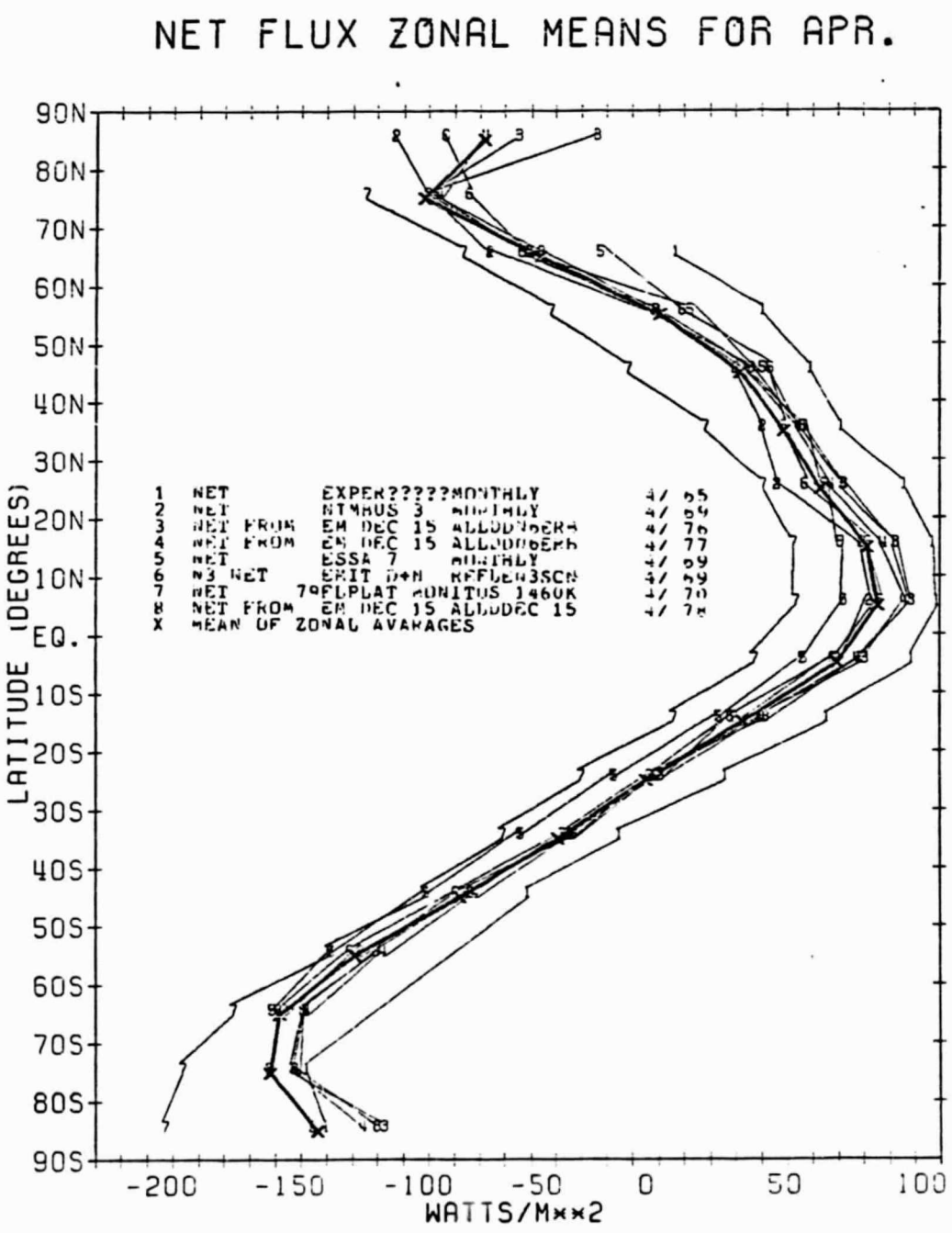
NET FLUX ZONAL MEANS FOR APR.
90N
80N
70N
60N
50N
40N
30N
20N
10N
EQ.
10S
20S
30S
40S
50S
60S
70S
80S
90S
LATITUDE (DEGREES)
-200
-150
-100
-50
0
50
100
WATTS/M**2
1 NET EXPER?????MONTHLY 4/ 55
2 NET NIMBUS 3 MONTHLY 4/ 64
3 NET FROM EM DEC 15 ALLDDDEC15 4/ 76
4 NET FROM EM DEC 15 ALLDDDEC15 4/ 77
5 NET ESSA 7 MONTHLY 4/ 69
6 N3 NET ERIT D+N REFLEN3SCN 4/ 69
7 NET 79FLPLAT MONITOR 1460K 4/ 70
8 NET FROM EM DEC 15 ALLDDEC 15 4/ 78
X MEAN OF ZONAL AVERAGES

Figure I-14

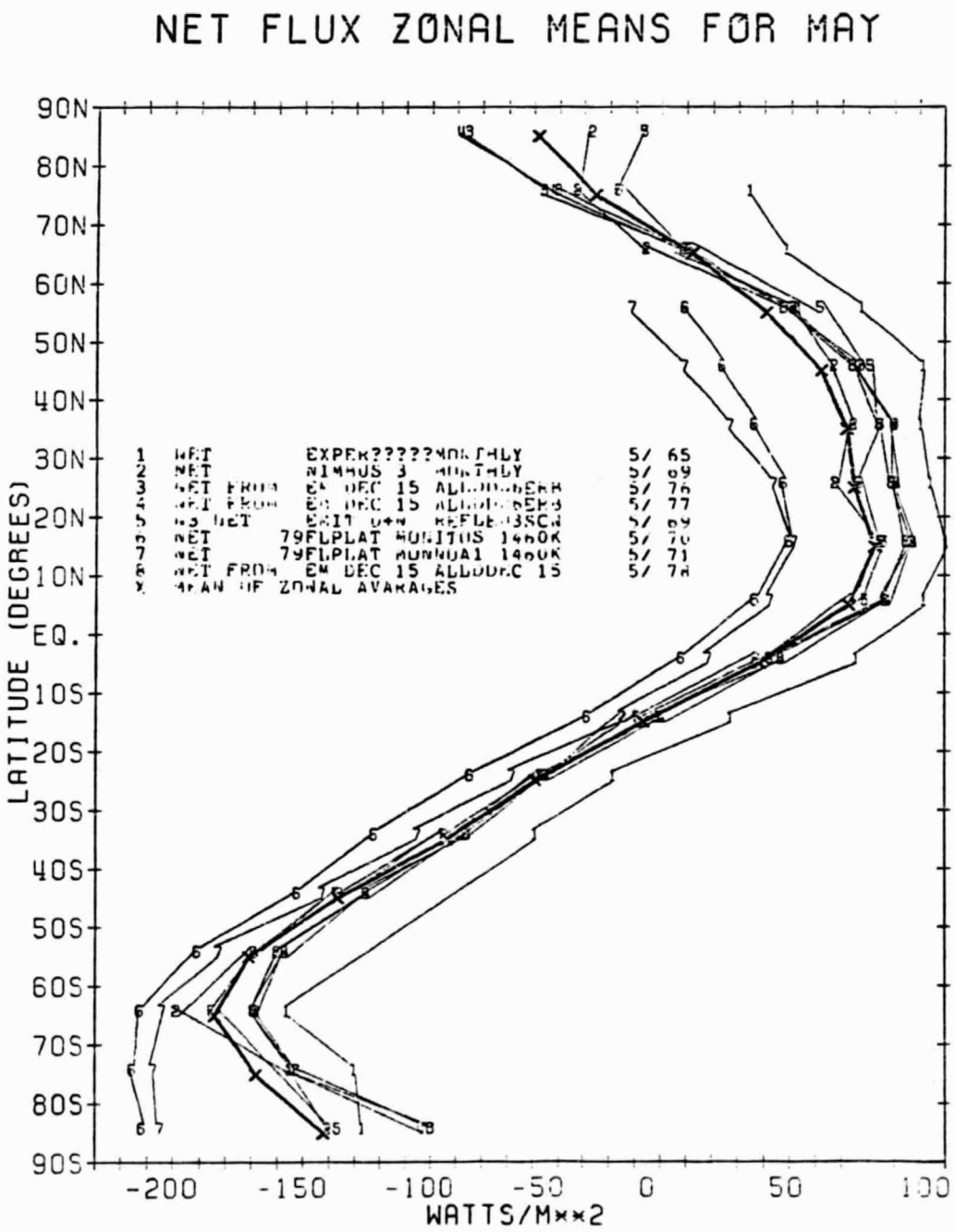
NET FLUX ZONAL MEANS FOR MAY
90N
80N
70N
60N
50N
40N
30N
20N
10N
EQ.
10S
20S
30S
40S
50S
60S
70S
80S
90S
LATITUDE (DEGREES)
-200
-150
-100
-50
0
50
100
WATTS/M**2
1 NET EXPER?????MONTHLY 5/ 65
2 NET NIMBUS 3 MONTHLY 5/ 69
3 NET FROM EM DEC 15 ALL 5/ 76
4 NET FROM EM DEC 15 ALL 5/ 77
5 NET 79FLPLAT MONTHS 14b0K 5/ 70
7 NET 79FLPLAT MONNDA1 14b0K 5/ 71
8 NET FROM EM DEC 15 ALL 5/ 78
X MEAN OF ZONAL AVARAGES

Figure I-15

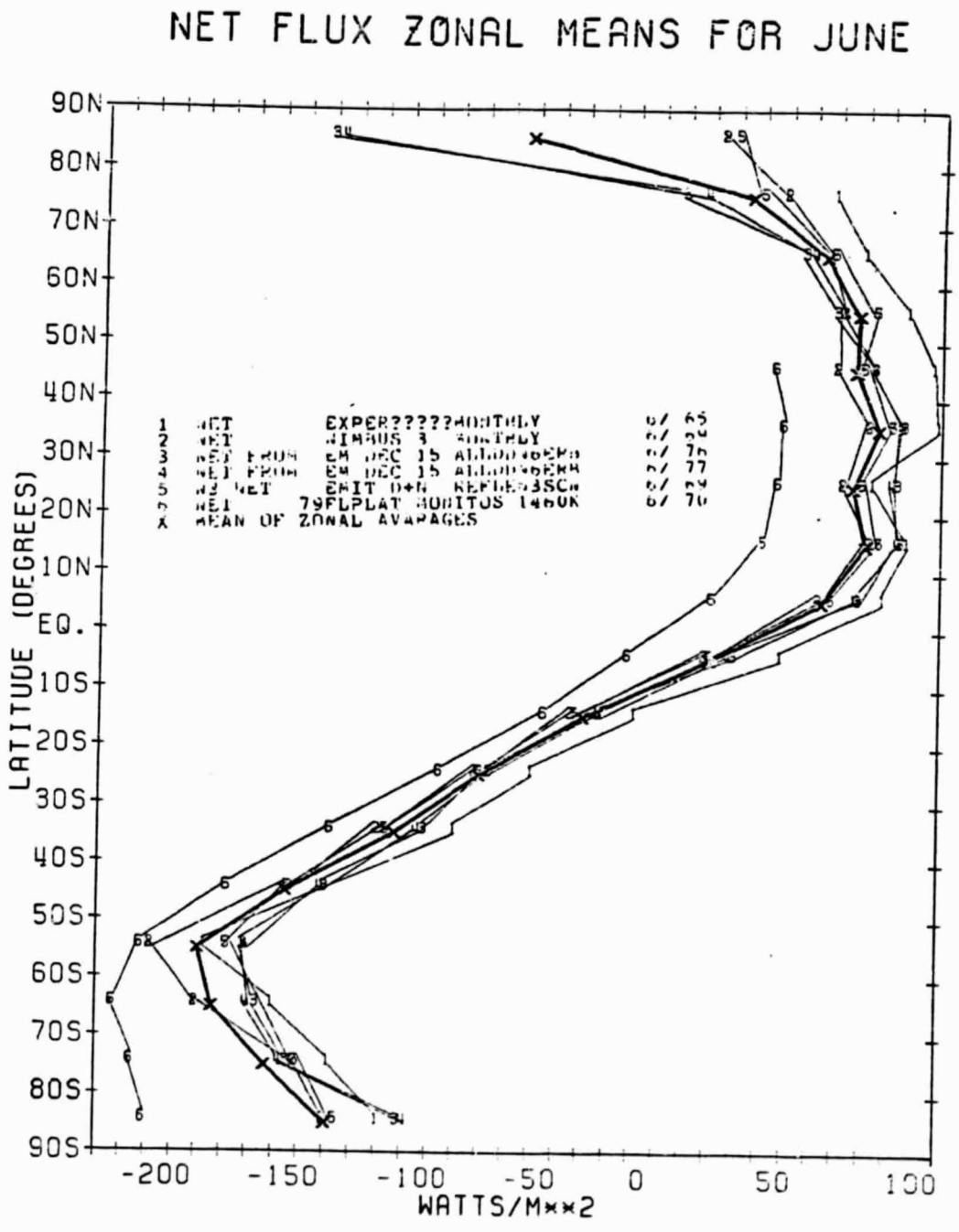

American weather anomalies, distinctly different from the preceeding and following years. Differences can be noted in the December-January zonal means for emitted and net fluxes for these years (Figures 1-16 and 17, respectively). The fact that the emitted flux (Figure 1-16) in Dec. 76 - Jan. 77 was larger at higher latitudes ($60^{o}N$ - $90^{o}N$) and lower at mid-latitudes ($30^{o}N$ - 90^{o})N in comparison to the other years may be indicative of the strong and persistent atmospheric "blocking" patterns which characterized this period in the Nothern Hemisphere. For under such blocking conditions, the increased meridional circulation would allow anomalous amounts of warm air to be advected into higher latitudes which, in turn, would result in increased longwave emission. Conversely, at mid-latitudes, the increase in cold air advection associated with the blocking flow would result in decreased longwave emission. Since the NCAR Community Climate Model (CCM) has recently replicated the blocking situation found over North America during the 1976/77 winter (Blackman, 1981), our model experiments planned for the remaining portion of the research period of this contract have additional impetus potential.

A more complete documentation of the new NIMBUS-6 results, as well as preliminary discussion, is in preparation (Ciesielski, Campbell, and Vonder Haar, 1981). This special report under the present contract will be patterned after Ellis and Vonder Haar (1976) and Campbell and Vonder Haar (1980).

2.0 Numerical Model Experiment Definition and Tests

Two complementary models are presently under development. The first is a statistical-dynamical model patterned after the recent work of Ashe (1979). It contains very crude vertical resolution (only two levels; but in principle, more can be added) and an arbitrary horizontal resolution. The horizontal dependence is represented by spectral components, which have recently been

Figure I-16

ORIGINAL PAGE IS
OF POOR QUALITY

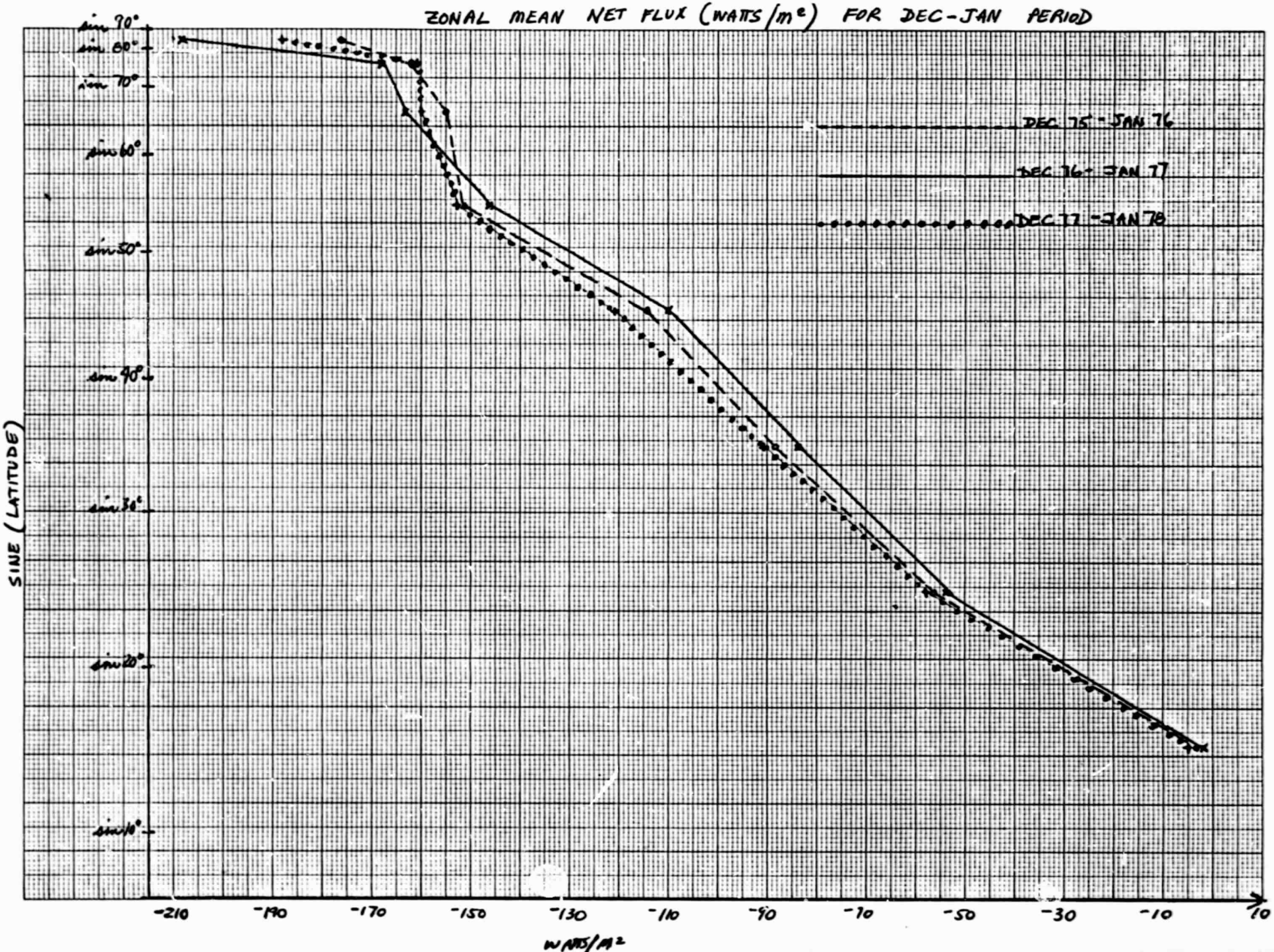
ZONAL MEAN NET FLUX (WATTS/m²) FOR DEC-JAN PERIOD
DEC 75 - JAN 76
DEC 76 - JAN 77
DEC 77 - JAN 78
SINE (LATITUDE)
sin 70°
sin 60°
sin 70°
sin 60°
sin 50°
sin 40°
sin 30°
sin 20°
sin 10°
-210
-190
-170
-150
-130
-110
-90
-70
-50
-30
-10
10
WATTS/M²

Figure I-17

demonstrated superior to a finite difference grid. Because the dissipation is often modeled by horizontal diffusion, it is useful to use spherical harmonics as the spectral basis functions.

In this first model approach, the diabatic forcing is assumed temporally constant (e.g., a seasonal average) and we solve for the steady circulation as a response. Transient motions (i.e., weather) are parameterized as dissipative to the steady circulation. To make the model tractable, the results understandable, and the energetics simple, a dynamical approximation to the primitive equations is assumed. At present the "linear balance" system is being used because it is the simplest quasi-geostrophic-type system which is valid globally. Despite the "linear balance" label, the vorticity and thermodynamic budgets are fully non-linear. This is the chief distinction from the generation of linear models (e.g., Sankar-Rao and Saltzmann) used in the 1960's; in those earlier studies, the mean zonal flow was specified a priori independent of the standing eddies. Hence, a large part of the general circulation was assumed, and not necessarily consistent relative to the eddies. Here we take the much more satisfying approach of finding both the mean flow and the standing eddies which result from a prescribed stationary forcing, consisting primarily of radiative heating/cooling, latent heat release, and sensible/latent heat flux from the surface.

Unfortunately, this important aspect of reality also makes the problem much more difficult to solve, because a non-linear system of equations must be solved. There is no universally applicable method for finding the non-linear solution; indeed, there is not even a guarantee of a unique solution or of any solution at all. Because of Ashe's results, we are confident that a solution can be obtained. At present, we are attempting three methods of solution:

(1) Iterate in time from a simple initial condition to the asymptotic steady state.

(2) Use a standard IMSL non-linear equation solver. (Unfortunately, this method depends crucially on initial conditions, which may not be sufficiently precise.)

(3) First calculate a linear response and then use this solution as the initial guess in the iterative methods (1) and/or (2).

We still have a significant amount of work to do in this area in order to obtain the non-linear solution. Because of the notorious difficulties with non-linear systems of equations, there is no guarantee of success.

The second model approach makes similar dynamic approximations, but explicitly calculates the time evolution of the flow. Thus, time-dependent radiation can be taken from observations (including the seasonal cycle and the interannual variation), applied as a forcing, and the response of the atmosphere computed. The individual "synoptic" flows can then be averaged to obtain monthly means, seasonal means, and interannual variations. Thus, we will be able to find whether or not the atmospheric circulation is sensitive to externally specified changes in radiative forcing. In turn, this will guide our understanding and interpretation of the present and future radiation budget measurements from satellites.

The preliminary development of the latter model is being done by Adel Hanna, a Ph. D. student, under the auspices of other funding sources. Duane Stevens is advising him in this research effort. As this model is in an early development stage, results are of a very preliminary nature. Further "tuning" of the physical parameterization will probably be required in order to attain an approximately veritable simulation of the annual average and seasonally-varying circulation. The following represents some of these preliminary results.

The second model under discussion is a two-level global "linear balance" model. In the horizontal domain a rhomboidal spectral truncation is assumed (presently, we truncate at zonal wave no. 9). In this section the results of time integration of the model up to 120 days, to simulate the January circulation, are discussed.

The model was initiated assuming an atmosphere at rest and with constant moist adiabatic lapse rate (6.5°/km). Assuming a perpetual January forcing, the solar inclination is fixed to that of the first of January. Figure 2-1 shows the net solar radiation at the top of the model's atmosphere and the net solar radiation absorbed by the earth's surface at different latitudes in the model. Except the Artic Ocean, sea surface temperature were prescribed as the January climatological values. Orographic effects are parameterized through the vertical motion at the 1000-mb level.

The winter observational estimations for different variables were taken from Newell et al. (1971). Data for the average January were taken from Oort and Rasmusson (1971).

a) The Average Zonal Wind

The zonal wind component at different grid points was averaged in latitude and time (30 days). In the northern hemisphere (winter hemisphere) the average 500-mb zonal wind compared well with the observed pattern (Figure 2-2). The same for the 250-mb distribution (Figure 2-3). The observations show a westerly jet at 30°N (20 m sec^{-1} at 500 mb and 38 m sec^{-1} at 250 mb). The calculated values place the maximum zonal wind at 23°N with maxima of 15 m sec^{-1} and 25 m sec^{-1} for the 500-mb and 250-mb cases, respectively. It can also be noticed that the calculated averages for the period 61-90 days show nearly the same values as the averages for the periods 91-120 days in the case of 500 mb, also the same agreement between the 31-60 days average and 91-120 days in

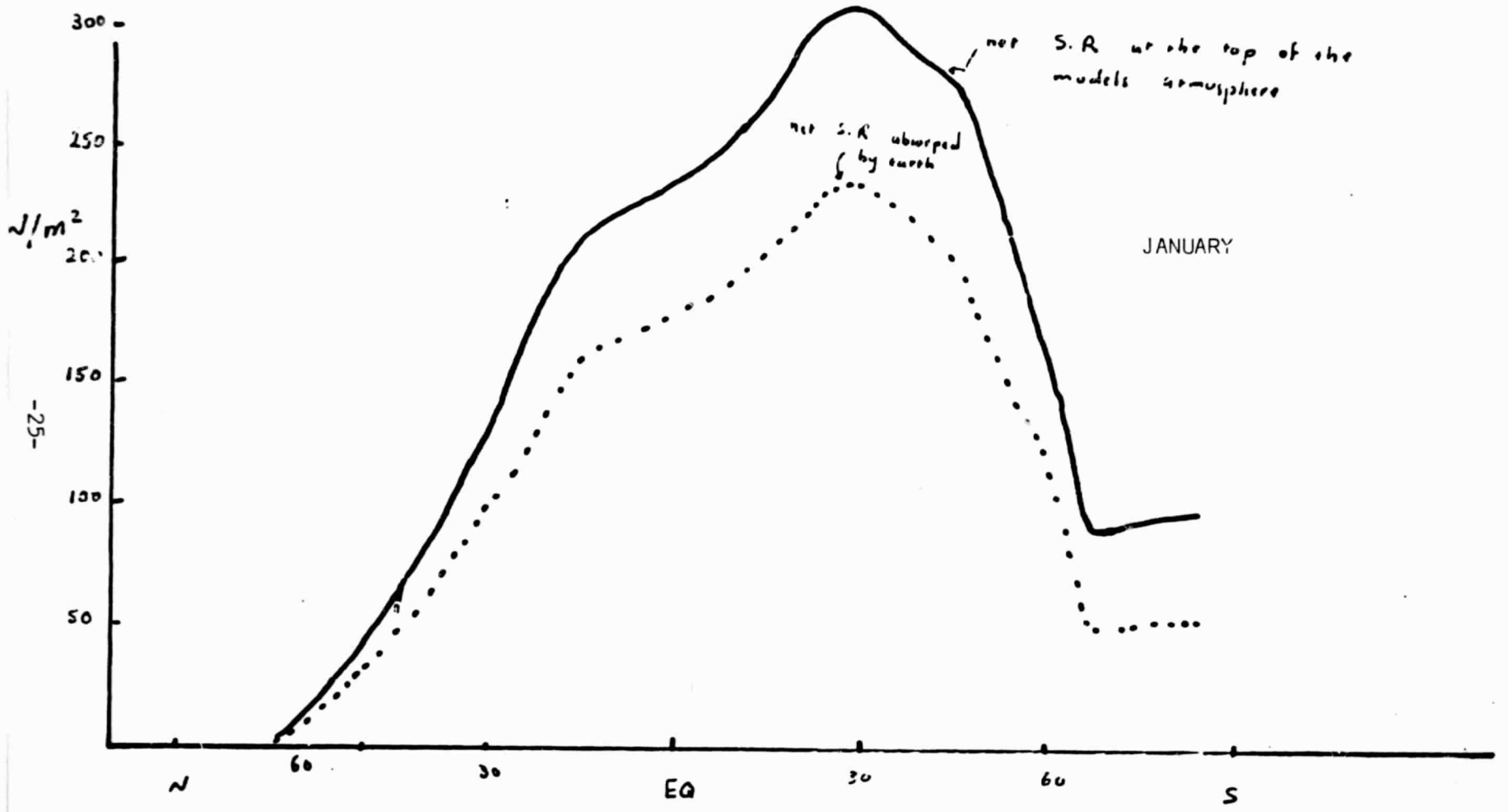

Fig. 2-1 Net Solar radiation at the surface and top of the model's atmosphere for January

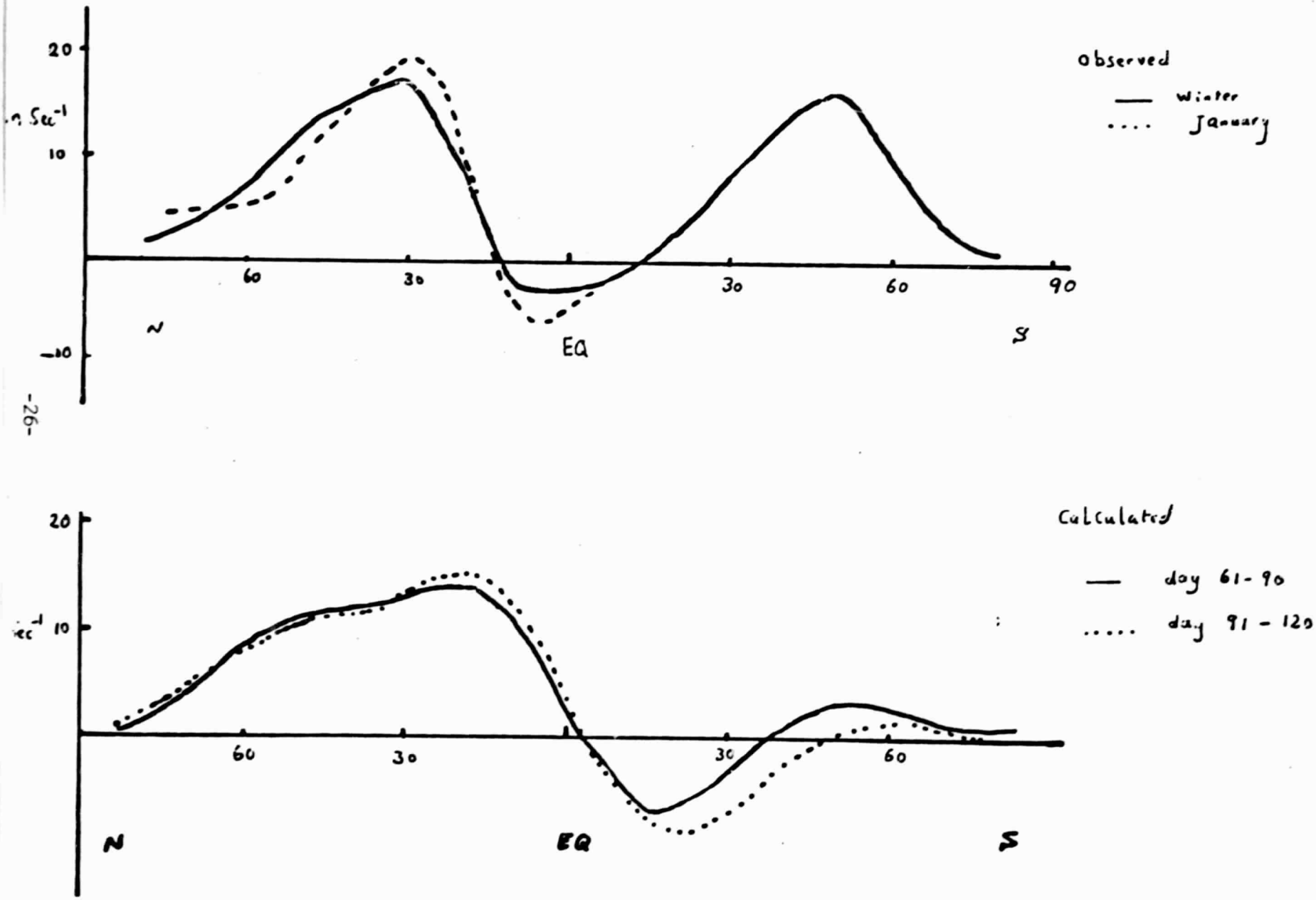

Fig. 2-2 Observed and calculated mean zonal wind 500 mb.

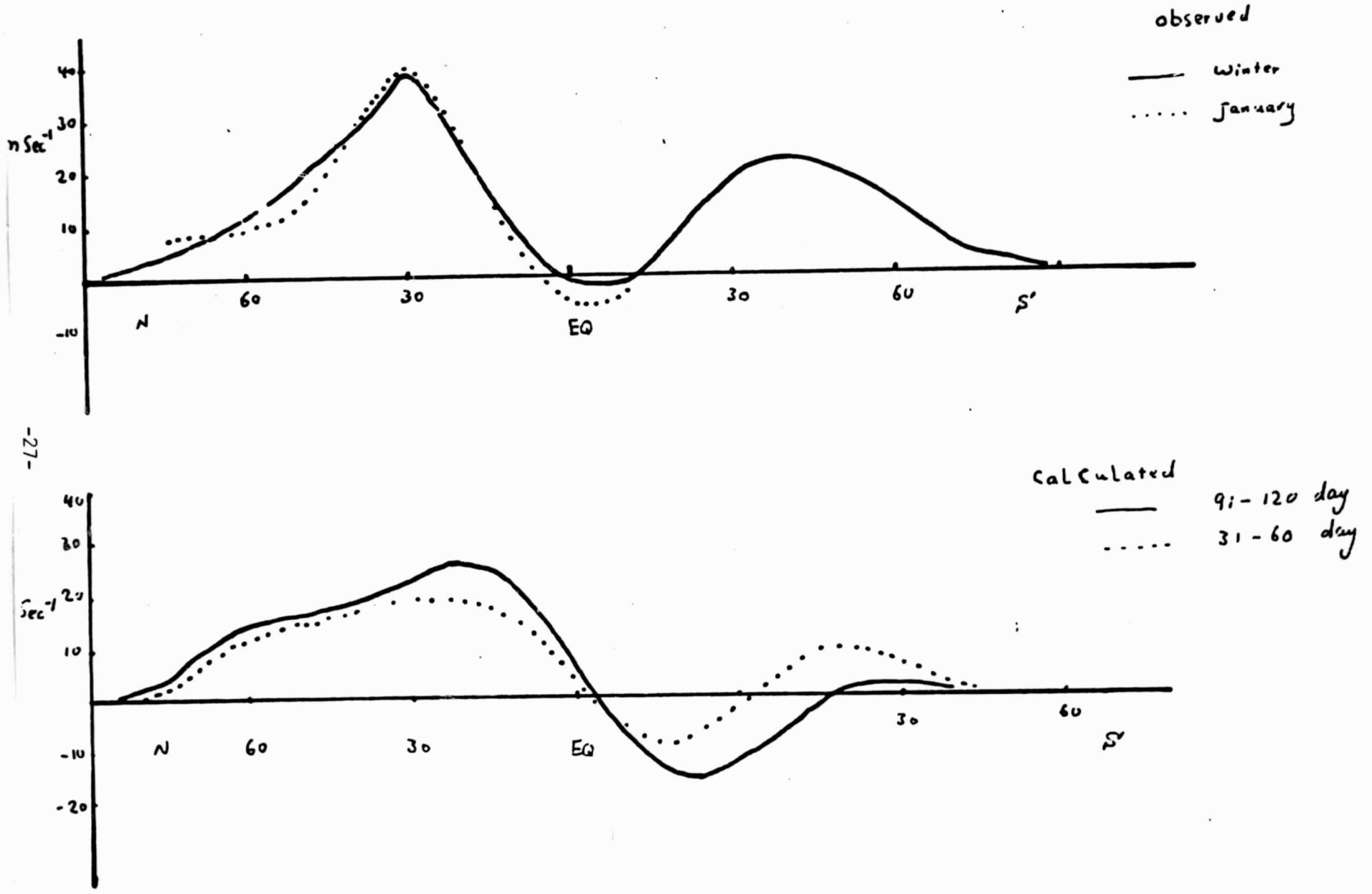

Fig. 2-3 Observed (200 mb) and calculated (250 mb) mean zonal wind.

the case of the 250 mb. This indicates that the zonal momentum is reaching a statistical steady state.

In the southern hemisphere (summer hemisphere) the calculated values have less agreement with observations than the northern hemisphere case. In both the calculated 500-mb and 250-mb cases, the westerly jet in the extratropical southern hemisphere is much damped and shifted. On the contrary, the equatorial easterlies are amplified and broadened to reach the southern hemisphere mid-latitudes. The variability between different time averages for both 500 mb and 250 mb may suggest that values at this region need a longer simulation than already have been done.

b) Meridional Wind Component

The zonally averaged meridional wind component is being calculated from the zonally-averaged velocity potential. The latter is at least one order of magnitude smaller than the velocity stream function (in middle and high latitudes). Even observational estimates show a large variability between winter and January cases (Figure 2-4). In the northern hemisphere the calculated averaged meridional velocity at 750 mb changes its sign corresponding to the vertical mass flux at 500 mb (Figure 2-4), validating the mass continuity. In the southern hemisphere the areas of equatorward flux (positive v) are not simulated since the vertical mass flux is mainly upward (negative w).

c) Vertical Velocity

The observed and calculated 500 mb vertical velocity field (units 10^{-4} mb sec^{-1}, 10^{-5} mb sec^{-1}, respectively) is shown in Figure 2-5. Again in the northern hemisphere the calculated values resemble the observed phase but with smaller amplitudes. The midlatitude ascending motions and the subtropical subsidence are well fitted with the observations. The calculated subtropical subsidence occurs in a rather broad latitude band in comparison to that which is observed. This feature may account for the same mass flux to counter the

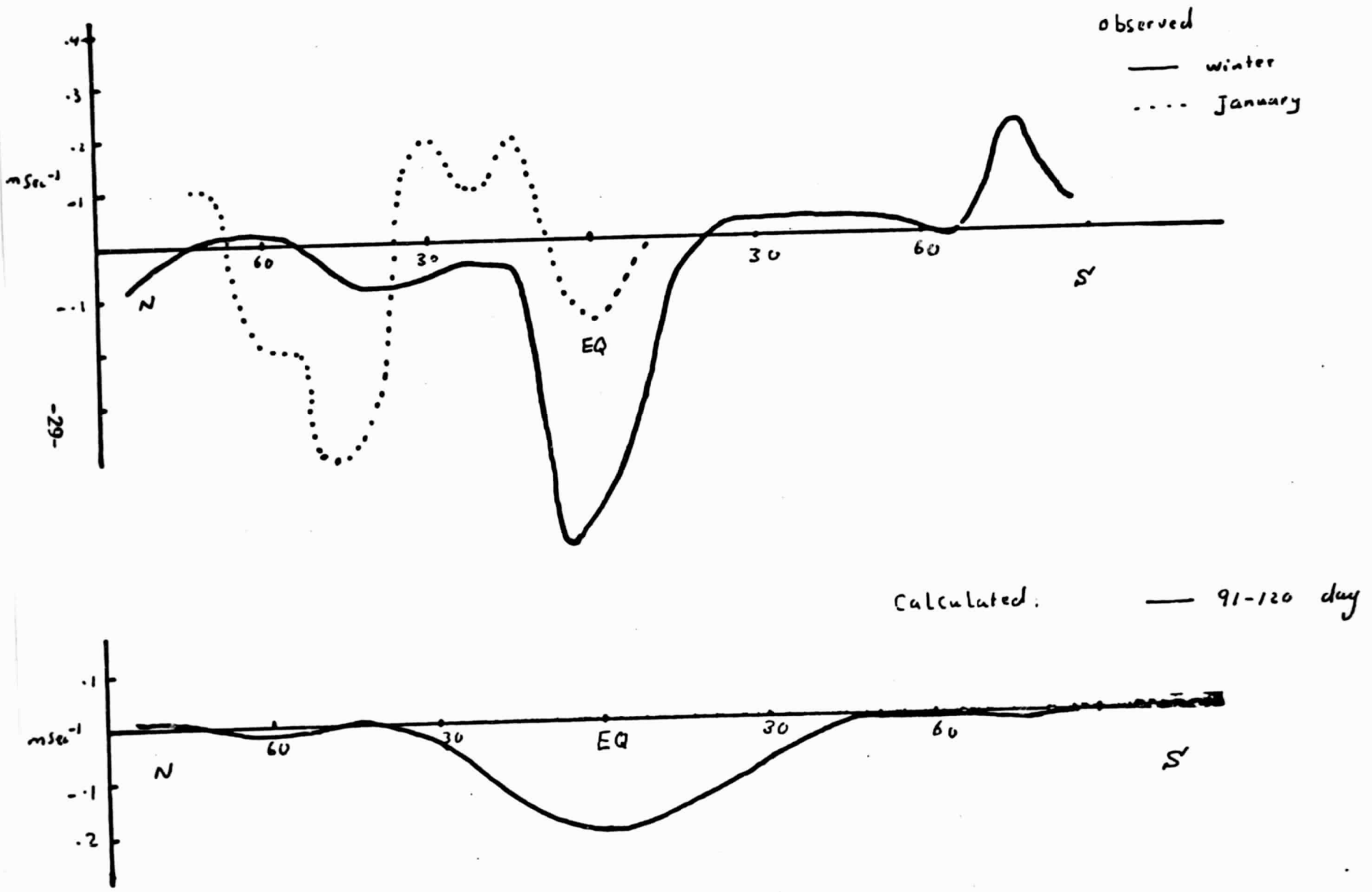

Fig.2-4 Observed(700 mb) and calculated(750 mb) mean meridional wind.

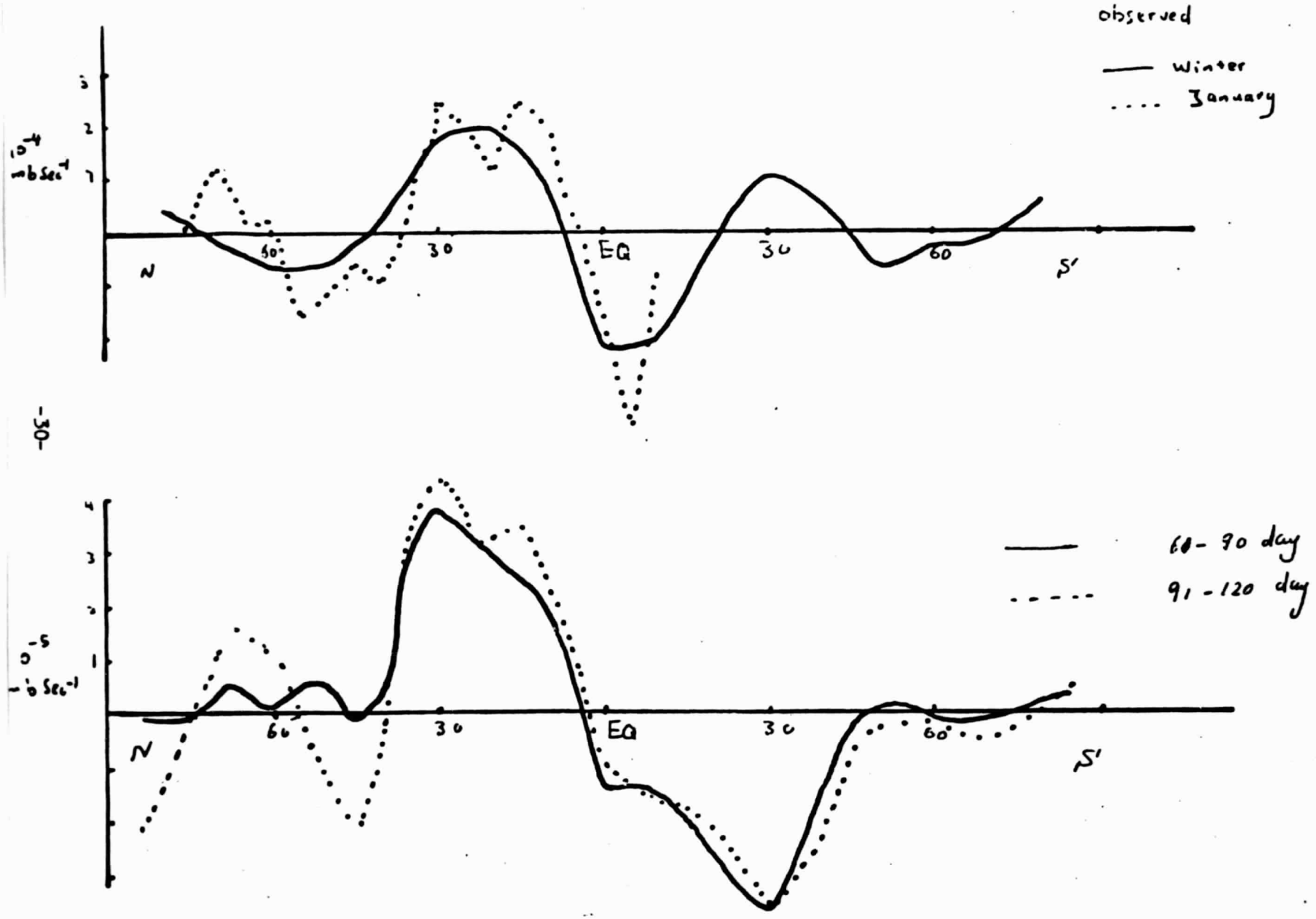

Fig. 2-5 Observed and calculated pressure velocity ω 500mb.

decrease of amplitude. In the southern hemisphere maximum shifting with the ITCZ is shifted to $30^{o}S$ with a very weak subsidence in the extratropical latitudes.

d) Moisture Budget

The model uses a simple moisture budget equation in the lower layer with the assumption that the upper layer is dry. Precipitation occurs with release of latent heat of condensation when the relative humidity of the lower layer exceeds 80%. The model's atmosphere is convectively adjusted if the temperature lapse rate, after the release of latent heat, exceeds the saturated adiabatic lapse rate. Figure 2-6 shows the zonally averaged precipitation and mixing ratio (gm/gm); both have a reasonable distribution except the subtropical maxima at $30^{o}N$. This is a result of the critical relative humidity assumed for precipitation (80%). At the subtropical latitudes the relative humidity may exceed 80% without any precipitation.

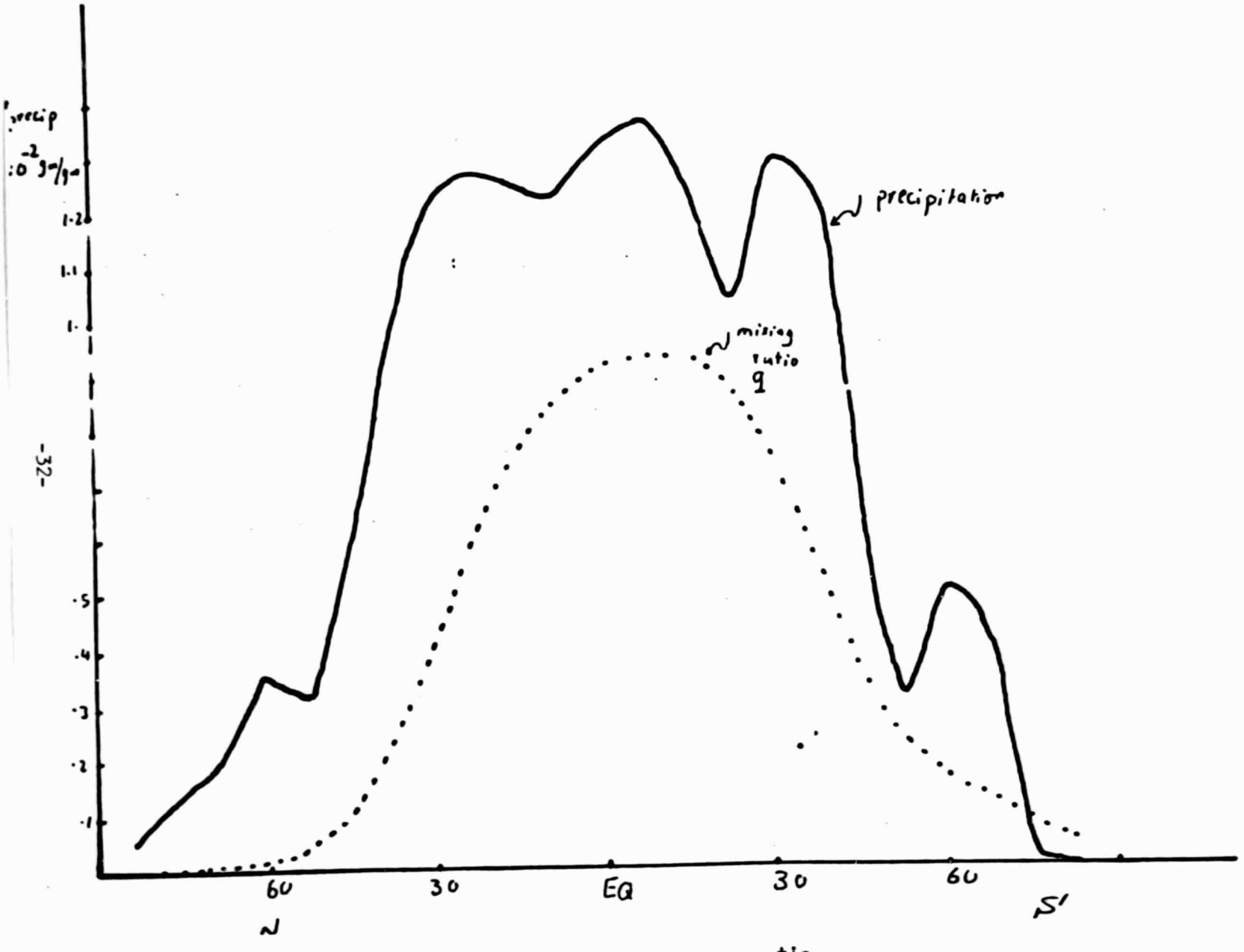

Fig. 2-6 Calculated precipitation and mixing ra day 91-120.

3.0 Review of Concurrent Radiation Budget Research by Other Scientists

During the last year new papers and reports by Ohring, G. Smith *et al.*, Gruber, Hansen *et al.*, and others have continued the study of earth radiation budget and related modeling. We are reviewing these papers as they relate to our work on this project. They will be referenced in our reports in preparation.

4.0 References

Ashe, S., 1979: A nonlinear model of the time-average axiliary asymmetric flow induced by topography and diabatic heating. J. Atmos. Sci., 36/1, 109-126.

Campbell, G. G. and T. H. Vonder Haar, 1980: An analysis of two years of NIMBUS-6 earth radiation budget observations: July, 1975 to June, 1977. Paper #320, Department of Atmospheric Science, Colorado State University, Fort Collins, CO.

Campbell, G. G., 1981: Energy transports within the earth's atmosphere ocean system from a climate point of view. Department of Atmospheric Science, Colorado State University, Ph. D. Dissertation

Cieslelski, P.G. G. Campbell and T. H. Vonder Haar, 1981: An analysis of NIMBUS-6 and NIMBUS-7 data as pertains to the earth radiation budget. In preparation.

Ellis, J. and T. H. Vonder Haar, 1976: Zonal average earth radiation budget measurements from satellites for climate studies. Atmospheric Science Paper #240, Colorado State University, Fort Collins, CO.

Newell, R. E., J. W. Kidson, D. G. Vincent and G. J. Boer, 1971: The general circulation of the tropical atmosphere and interactions with extratropical latitudes. Vol. 1.

Oort, A. H. and E. M. Rasmusson, 1971: Atmospheric circulation statistics, NOAA Professional Paper 5, 323 pp. U. S. Government Printing Office, Washington, D. C.

Stephens, G., G. G. Campbell, and T. H. Vonder Haar, 1981: Earth radiation budgets. J. Geoph. Res., 86, 9739-9760.